Pentagons and Heptagons in the First Water Layer on Pt(111)

S. Nie,[1] Peter J. Feibelman,[2] N. C. Bartelt,[1] and K. Thürmer[1]
[1]*Sandia National Laboratories, Livermore, California 94550, USA*
[2]*Sandia National Laboratories, Albuquerque, New Mexico 87185, USA*
(Received 14 April 2010; published 9 July 2010)

Scanning tunneling topography of long-unexplained "$\sqrt{37}$" and "$\sqrt{39}$" periodic wetting arrangements of water molecules on Pt(111) reveals triangular depressions embedded in a hexagonal H_2O-molecule lattice. Remarkably, the hexagons are rotated 30° relative to the "classic bilayer" model of water-metal adsorption. With support from density functional theory energetics and image simulation, we assign the depressions to clusters of flat-lying water molecules. 5- and 7-member rings of H_2O molecules separate these clusters from surrounding "H-down" molecules.

DOI: 10.1103/PhysRevLett.105.026102 PACS numbers: 68.55.−a, 64.60.qj, 68.37.Ef, 68.43.Hn

The broad importance of water-materials interactions in nature and technology underlies substantial literature devoted to wetting [1,2]. Numerous metal single-crystal surfaces are known to support a two-dimensional water layer. According to Young's equation, that proves they are more attractive to water than water is to itself.

Nonetheless, wetting is understood in only a few cases [2,3]. One reason is that experimental determinations of wetting-layer molecular arrangements are difficult, and correspondingly rare. Another is that systematic error in state-of-the-art modeling tools, whether first principles or semiempirical, leaves their structural implications open to question, more so when energy differences are relatively small—as in wetting.

With Pt electrodes at the heart of many electrochemical applications, notably fuel cells, the affinity of H_2O for Pt(111) is of particular interest. Still, although the $\sqrt{37} \times \sqrt{37}$-$R25.3°$ and $\sqrt{39} \times \sqrt{39}$-$R16.1°$ periodicities of the low-energy complete-wetting phases on this surface have been known for more than a dozen years [4], their molecular structure has remained a mystery.

New, high-resolution scanning tunneling microscope (STM) images of these structures now provide clues. Following them, with the use of density functional theory (DFT) energy minimization and STM image simulation, we propose H_2O-molecule arrangements for both the $\sqrt{37}$ and $\sqrt{39}$ wetting phases unlike any previously imagined. The common bonding motif is a cluster of flat-lying molecules enabled to lie especially close to Pt atoms by H_2O-molecule pentagons and heptagons surrounding them.

Conventionally, the first wetting layer on a close-packed metal surface (the "classic bilayer") is a single (0001) sheet of ice-Ih, strained to achieve $\sqrt{3} \times \sqrt{3}$-$R30°$ periodicity. Of the two water molecules in its unit cell, one lies almost parallel to the metal surface, binding to it through an oxygen lone-pair orbital, and the other lies several tenths of an Å higher, contributing one O-H bond to the layer's H-bond network, while the other dangles into the vacuum [1]. To account for their first observation of the $\sqrt{37}$ and $\sqrt{39}$ periodicities on Pt(111) with He diffraction, Glebov *et al.* modified this picture only slightly [4]. They attributed their observations to icelike sheets of water molecules, rotated and compressed to fit in $\sqrt{37} \times \sqrt{37}$-$R25.3°$ and $\sqrt{39} \times \sqrt{39}$-$R16.1°$ supercells.

Why, however, should the structure of Glebov *et al.* have low energy? The unrotated, uncompressed $\sqrt{3}$ phase is in itself not a particularly low-energy state. Rotation and compression to form a $\sqrt{37}$ or $\sqrt{39}$ moiré make matters worse because now only a relatively small number of flat-lying molecules can be in a low-energy configuration atop a Pt atom [5]. Logic or not, there is also no experimental evidence for such moiré structures. One might hope to find it in high-resolution images, but previous STM experiments [6] did not turn up $\sqrt{37}$ and $\sqrt{39}$ wetting phases—hence, our own study.

We conducted ice growth and STM characterization in an ultrahigh-vacuum chamber with base pressure 4×10^{-11} mbar. Films were grown by directing water vapor onto Pt(111) at 140 K. The pressure during deposition was typically 2×10^{-9} mbar. STM measurements were performed at $T < 115$ K. To avoid tip-induced damage, we kept the tunneling current <1 pA. Tip voltage was between 0.2 and 1 V. We determined the crystallographic directions of the Pt(111) substrate by evaluating the registry of atomic positions on both sides of an atomic Pt step [7]. All STM images presented herein are oriented in the same way relative to the substrate.

Figure 1(a) shows the structure of two-dimensional wetting-layer islands, which form at low coverage (with islands covering about half the Pt surface.) The striking feature is the disordered arrangement of dark triangular regions. The depressions appear to lie ~0.3 Å below the bright water rings, compared to an apparent step height of 1 Å at the step edges of the water layer under the same imaging conditions. Surrounding the triangular depressions are hexagonal rings of water molecules, which are rotated approximately 30° relative to expectation based on the classic $\sqrt{3}$ bilayer. The rotation is evident in Fig. 1(b) where (at the upper right) a small domain of $\sqrt{3}$ oriented water appears.

Although the disordered structure in Fig. 1(a) is typical of as-grown films, occasionally we find ordered patches of the triangular features [see Fig. 1(c)], whose periodicity and rotation are precisely that of the $\sqrt{37}$ phase. Understanding the $\sqrt{37}$ structure thus amounts to deciphering and interpreting the structure of the dark triangles.

The very center of each triangular depression is particularly dark, whereas a continuation of the outer hexagonal network would place a water molecule there. Thus a complete network of hexagonal rings as proposed in previous models [4] cannot be correct.

A satisfactory alternative should adhere to the basic principles that a wetting structure is better bound if the O atoms of more of its flat-lying water molecules are in or near atop sites, if its flat-lying molecules are clustered, so that their O atoms are minimally hindered from approaching the metal (cf. Haq *et al.* [8]), and if few, or optimally *no*, H bonds are broken.

With a complete hexagonal network inconsistent with experiment, the last constraint forces us to attribute the dark triangles to topological defects. The area of the triangles suggests they contain 6 H_2O molecules. If these molecules can lie flat, such that their O atoms lie directly above 6 metal atoms, then the 1st and 2nd constraints are also satisfied. Thus, energetic constraints guide us to interpret the dark triangles as di-interstitial defects [cf. Fig. 2(a)], wherein a six-molecule hexagonal ring, rotated relative to the surrounding ones, replaces four molecules of the undisturbed hexagonal mesh [9].

The ring's empty center and the center of a triangle depression coincide. Thus, the dark spot in STM is explained naturally. The dark vertices of the triangles seen in Fig. 1 correspond to heptagon centers. There are two possible orientations of the triangle, corresponding to those of the substituted four-molecule cluster drawn as dark (red) dots in Fig. 2(a). Triangles of both orientations are observed experimentally in Fig. 1(a).

Figure 2(b) makes clear how all three principles are also satisfied. Twelve of the 13 flat-lying H_2O molecules in the $\sqrt{37}$ unit cell are clustered in a central hexagon with O atoms in atop sites, and another hexagon surrounding it. No H bond is broken. The puzzle of the 30° rotation is resolved because the rotated hexagons consist primarily of H-down molecules, which experience corrugation of the substrate only weakly. Thus, rotation of the H-down region of the wetting phases relative to the central flat H ring is not a serious impediment to formation of the defect structure.

Remaining issues require support from calculations. One is why only the molecules in the central hexagonal ring seem close to the metal surface. Another is whether the strain-energy price is prohibitive of accommodating the di-interstitial with relatively short inter-H_2O separations at the borders of the depressions.

We addressed these concerns with first-principles binding-energy calculations, and STM image simulations, using the VASP DFT code [10], the Perdew-Burke-Ernzerhof (PBE) version of the generalized gradient approximation [11], and the projector-augmented wave approximation [12,13]. We modeled the Pt(111) substrate as a 3-layer slab, with water adsorbed on top of it. Atoms of the lowest metal layer were fixed in theoretical bulk Pt relative positions ($a_{\mathrm{PBE}} = 3.98$ Å); all other atom posi-

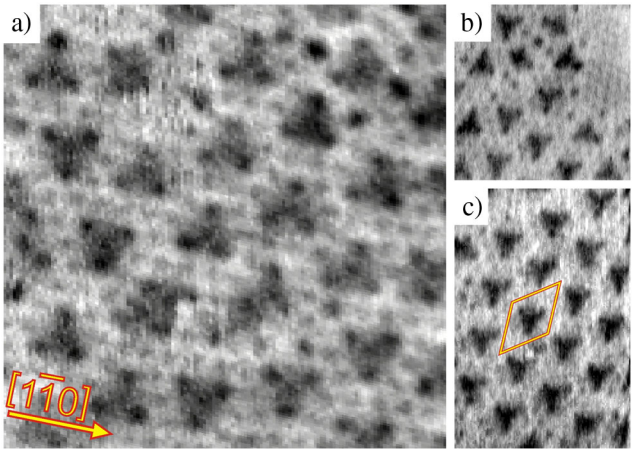

FIG. 1 (color online). STM images of submonolayer water deposited on Pt(111) at 140 K. (a) Disordered arrangement of triangular depressions (8 nm × 8 nm, $V_{\mathrm{tip}} = 0.5$ V, $I_t = 1$ pA), (b) region adjacent to disordered triangles (7 nm × 7 nm, $V_{\mathrm{tip}} = 0.2$ V, $I_t = 1$ pA). (c) An ordered region (7 nm × 10 nm, $V_{\mathrm{tip}} = 0.2$ V, $I_t = 1$ pA).

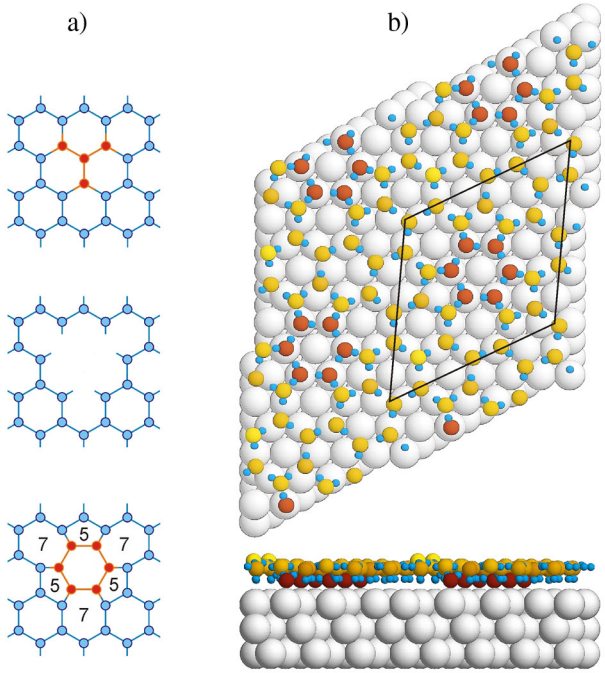

FIG. 2 (color online). (a) Schematic showing the formation of a "575757" di-interstitial defect in a hexagonal lattice. (b) Model for the $\sqrt{37}$ phase of water on Pt(111) incorporating this defect. The atomic positions have been relaxed with DFT. Shades ranging from light (yellow) to dark (brown) indicate the relative heights of the oxygen atoms.

tions were relaxed till forces on them were <0.045 eV/Å in magnitude. For accuracy, we used a 700 eV plane-wave basis cutoff, and sampled the $\sqrt{37} \times \sqrt{37}$-$R25.3°$ surface Brillouin zone with a 3×3 set of equally spaced k vectors. We accelerated electronic relaxation through Methfessel-Paxton Fermi level smearing [14] (width = 0.2 eV). Neugebauer-Scheffler [15] corrections canceled unphysical fields associated with the periodic slab repeats. Generally, dangling H bonds were started pointing toward the metal prior to optimization. Flipping them up always increased the system energy.

The relaxed $\sqrt{37}$ unit cell with the di-interstitial is shown in Fig. 2(b). This structure is superimposed on the STM images in Figs. 3(a) and 3(b). A STM image simulation based on the DFT electron density is shown in Fig. 3(c). Plotted there, for comparison with STM images acquired with a 0.2 V bias, is the height above the Pt surface of a constant electron-density contour (3.2×10^{-7} $e/\text{Å}^3$) attributable to electrons from the Fermi level to 0.2 eV below.

There are 26 H_2O molecules in the unit cell, with 12 in a central hexagon and another hexagon surrounding it. Remarkably, the molecules of the outer hexagon are rather high, consistent with experiment, and tilted out of the surface plane. They thereby bridge the central hexagon and the remaining water molecules, whose dangling H bonds force them to lie higher. The result is that the O-Pt separations of the central molecules optimize to just 2.24 Å. That betokens strong binding, compared to the 2.68 Å we find for the flat-lying molecules in a classic $\sqrt{3}$ H-down bilayer (or 2.87 Å for H-up). Notice that the O-O distances in the "575757" defect projected onto the surface plane are shorter than those in the surrounding hexagons. This result is consistent with experiment, as the overlay in Fig. 3(a) shows. Also consistent is that all the O atoms away from the low hexagon lie roughly at the same height above the metal (apart from the slightly higher isolated flat-lying molecule).

Note the good correspondence between the simulated image and the STM images of Fig. 1, and, in particular, of the size of the dark triangles. The charge contour shown has the H-down H_2O molecules 0.6 Å above the central flat-lying molecules and 1.5 Å above clean Pt, roughly consistent with experiment. Contours of smaller charge density would likely improve agreement but are problematic for DFT.

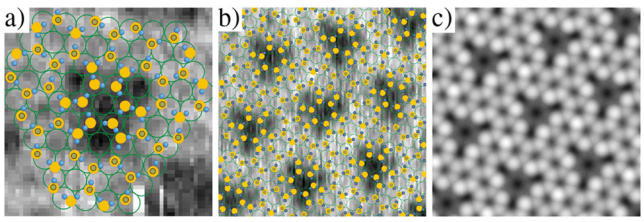

FIG. 3 (color online). Overlay of the molecular model on STM images of (a) a single triangle and (b) an ordered $\sqrt{37}$. Panel (c) shows a simulated STM image based on DFT charge densities.

So, DFT shows that the relaxed defect structure agrees with experiment. But is it lower in energy than competing structures with no defect? Indeed yes: our calculations for the di-interstital arrangement yielded a lattice binding energy of 0.55 eV/H_2O [16]. This is higher (i.e., more stable) than for any hexagonal H_2O network we have considered. Specifically, it is 0.10 eV higher than for the conventional $\sqrt{3}$ H-down bilayer and 23 meV per molecule higher than for a version of the moiré structure proposed by Glebov *et al.* rearranged so that as many as possible of its flat-lying water molecules occupy near-atop sites.

Importantly, the di-interstitial structure has much lower energy than arrangements in conflict with even just one of the three constraints mentioned earlier. For example, if the H-bond arrangement is altered so that six H-down (instead of flat-lying) molecules surround the central hexagonal ring, violating the clustering constraint, the energy rises by 34 meV per water. For another, if the dark triangles are attributed to tetravacancies [17], there are six broken H bonds per unit cell [see Fig. 2(a), middle panel]. The binding energy of such a low-coverage arrangement is accordingly 70 meV per molecule worse than that of the di-interstitial structure.

Consider now the higher coverage $\sqrt{39}$ phase, which exists in equilibrium with 3D ice islands [18,19]. A $\sqrt{39}$ unit cell incorporating the "575757" defect is shown in Fig. 4(a). Slightly denser than the $\sqrt{37}$ (26 over 37), as required, it contains 28 water molecules over 39 Pt atoms. There are now two flat-lying molecules not directly linked to the "575757" structure. Positioning them together, as in Fig. 4(a), allows one to relax into an energetically preferred atop site.

DFT calculations for this phase imply an adsorption energy just a few tenths of a meV below that for the $\sqrt{37}$ and, again, significantly higher than the competing moiré proposed by Glebov with 32 molecules per unit cell. The relaxed configuration [see Fig. 4(a)] is similar to the $\sqrt{37}$, except that the isolated flat-lying water molecule over the atop site now lies low, only 2.21 Å above the Pt.

It is more difficult to compare this computed structure directly with STM measurements because the conditions for high-resolution imaging destroy the 3D islands that coexist with the $\sqrt{39}$ phase [7], scattering their water molecules nearby. The scattered water molecules tend to obscure the wetting-layer structure. Still, we did obtain images with $\sqrt{39}$ periodicity and dark triangular features, as shown in Figs. 4(b) and 4(c). Notice the adjacent footprints of 3D islands, disrupted during scanning.

Between the triangular depressions in the STM images, note bright areas of various sizes in apparent conflict with the model of Fig. 4(a), which has a low-lying molecule in the same position and thus "should be" dark [20]. Might they represent water molecules adsorbed on top of the $\sqrt{39}$ arrangement of Fig. 4(a), near its isolated flat-lying mole-

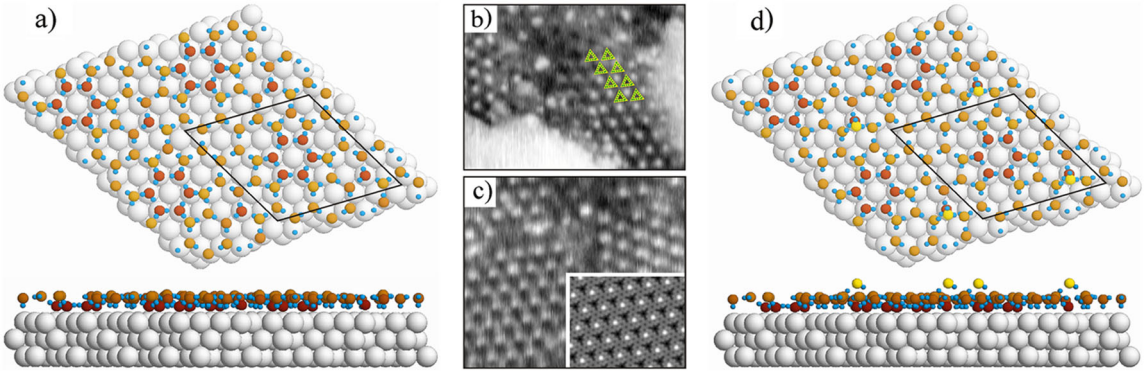

FIG. 4 (color online). (a) Schematic of the $\sqrt{39}$ structure. (b) STM image showing the coexistence of 3D crystallites with $\sqrt{39}$ (22 nm $\times$ 17 nm, $V_{\text{tip}} = 0.5$ V, $I_t = 5$ pA). Yellow triangles mark the triangular depressions. (c) STM image showing the two rotational domains (20 nm $\times$ 17 nm, $V_{\text{tip}} = 0.5$ V, $I_t = 1$ pA). (d) Relaxed configuration of a water molecule added on top of the structure in (a). Inset in (c) is an STM image simulation of the structure containing this molecule.

cules? To check (cf. Ref. [21]), we optimized such ''2nd-layer'' molecules. In the postrelaxation configuration of Fig. 4(d), their adsorption energy, 0.55 meV, equals that of the first layer, suggesting they could be part of the equilibrium structure that coexists with the 3D islands. (Experimentally, it is difficult to distinguish an equilibrium feature from one produced by 3D island disruption.) The simulated image in the inset of Fig. 4(c), made by integrating the DFT charge density from the Fermi energy to 0.5 eV below, and plotting a charge contour of $5 \times 10^{-7}\ e/\text{Å}^3$, reproduces the general appearance of the bright features seen experimentally.

In assessing the foregoing, note that although our DFT calculations do provide reasonable STM image simulations, and do account for the low energies of the observed structures compared to the classic bilayer, they do not yet explain two-dimensional wetting [7,18,19]. Specifically, the calculated lattice energy per molecule in the wetting layer is some 90 meV less than for bulk ice. Thus, H_2O/Pt(111) is yet another example showing that the accuracy of today's DFT needs improvement before we can rely on it to predict water-solid interactions.

Notwithstanding this caveat, we have offered herein evidence that the first wetting layer on Pt(111) is a mixture of 5-, 6-, and 7-membered rings of water molecules, favored by the energy gained when a perfectly H-bonded array of water molecules allows a significant fraction of them to lie close to 1st layer metal atoms. This structural difference compared to the classic, icelike bilayer has consequences for further water growth; notably, it suggests that 3D islands will not grow on top of the wetting layer, without substantial molecular rearrangement. More broadly, it underlines the importance of directly characterizing the first stages of water adsorption before claiming that one understands how water interacts with solids [22].

This work was supported by the DOE Office of Basic Energy Sciences, Division of Materials Sciences and Engineering, under Contract No. DE-AC04-94AL85000. P. J. F. acknowledges useful discussions with the group of T. Michely and the receipt of high-resolution STM images of the $\sqrt{37}$ and $\sqrt{39}$ phases after the model presented here was developed.

[1] M. A. Henderson, Surf. Sci. Rep. **46**, 1 (2002).
[2] A. Hodgson and S. Haq, Surf. Sci. Rep. **64**, 381 (2009).
[3] P. J. Feibelman, Phys. Today **63**, No. 2, 34 (2010).
[4] A. Glebov *et al.*, J. Chem. Phys. **106**, 9382 (1997).
[5] A. Michaelides *et al.*, Phys. Rev. Lett. **90**, 216102 (2003).
[6] M. Morgenstern *et al.*, Z. Phys. Chem. (Muenchen) **198**, 43 (1997).
[7] K. Thürmer and N. C. Bartelt, Phys. Rev. B **77**, 195425 (2008); Phys. Rev. Lett. **100**, 186101 (2008).
[8] S. Haq *et al.*, Phys. Rev. B **73**, 115414 (2006).
[9] Graphitic carbon has similar low-energy divacancy defects; see R. G. Amorim *et al.*, Nano Lett. **7**, 2459 (2007).
[10] G. Kresse and J. Furthmüller, Comput. Mater. Sci. **6**, 15 (1996); Phys. Rev. B **54**, 11 169 (1996).
[11] J. P. Perdew, K. Burke, and M. Ernzerhof, Phys. Rev. Lett. **77**, 3865 (1996).
[12] P. E. Blöchl, Phys. Rev. B **50**, 17 953 (1994).
[13] G. Kresse and D. Joubert, Phys. Rev. B **59**, 1758 (1999).
[14] M. Methfessel and A. T. Paxton, Phys. Rev. B **40**, 3616 (1989).
[15] J. Neugebauer and M. Scheffler, Phys. Rev. B **46**, 16 067 (1992).
[16] ''Lattice energy'' excludes zero-point contributions.
[17] S. Standop, A. Redinger, M. Morgenstern, T. Michely, and C. Busse, arXiv:1004.5030v1.
[18] S. Haq, J. Harnett, and A. Hodgson, Surf. Sci. **505**, 171 (2002).
[19] G. A. Kimmel *et al.*, J. Chem. Phys. **126**, 114702 (2007).
[20] Such low-lying flat molecules explain the small dark features away from the triangular depressions in Fig. 1(a).
[21] E. R. Batista and H. Jonsson, Comput. Mater. Sci. **20**, 325 (2001).
[22] See J. Carrasco *et al.*, Nature Mater. **8**, 427 (2009) for another example of pentagonal arrangements of water molecules.